Spectroscopy of plasmon anisotropy in wedge-shaped Au nanoclusters on (001) GaP surface

© V.L. Berkovits[1], V.A. Kosobukin[1], P.A. Alekseev[1], S.A. Khakhulin[2], A.V. Nashchekin[1]

[1] Ioffe Institute,
194021 St. Petersburg, Russia
[2] St. Petersburg State Electrotechnical University „LETI",
197022 St. Petersburg, Russia

E-mail: vladimir.berkovits@mail.ioffe.ru

Received May 5, 2026
Revised June 17, 2026
Accepted June 17, 2026

By annealing ultrathin gold films on the oxidized (001) surface of *n*-GaP crystal, Au nanoclusters were created in the form of wedges facing the crystal and extended in the [110] direction on the GaP surface. Using polarized light reflectance spectroscopy methods, the frequency and polarization anisotropy of plasmons localized on gold nanoclusters were studied. Spectral feature observed at energy of 1 eV is associated with dipole plasmons of Au clusters, polarized in [110] direction of GaP substrate. Another feature — at the energy of 2 eV — is due to plasmons with polarization in the orthogonal direction $[1\bar{1}0]$. Plasmon spectra of random anisotropic Au nanoclusters in Au/GaP(001) structures are explained theoretically taking into account the inhomogeneous broadening of plasmon lines similar to the spectra of Au/GaAs(001).

Keywords: gold nanoclusters, gallium phosphide, polarization spectroscopy, anisotropic plasmons.

DOI: 10.61011/SC.2026.05.63992.9501

1. Introduction

Fabrication and investigation of composite optical materials (metamaterials) based on semiconductors and noble metals are relevant to applications in nanophotonics, microelectronics, and related fields. One research direction involves structures and metamaterials based on $A^{III}B^{V}$ semiconductors and gold nanoclusters with high-quality-factor plasmon resonances. For example, three fundamentally different types of anisotropic gold clusters [1,2] have been produced by annealing thin Au films on GaAs(001) surfaces with different chemical states. In particular, wedge-shaped clusters consisting of a mixture of gold and the intermetallic compound Au_2Ga were observed [2]. These clusters result from the chemical interaction of Au with the GaAs substrate at its surface, whose crystallography determines the chemical composition, shape, and orientation of the nanoclusters [1–3]. According to Ref. [3], polyhedral Au clusters can also be expected to form on other gallium-containing $A^{III}B^{V}$ semiconductors. Furthermore, Ref. [4] reported silver clusters with planar faces embedded in a silicon crystal under different physicochemical conditions.

Here we describe the fabrication and properties of anisotropic Au clusters on the (001) surface of an *n*-GaP crystal. Wedge-shaped Au nanoclusters were produced by annealing a gold film on GaP(001), characterized, and studied by polarized optical reflectance spectroscopy; the resulting plasmon spectra were measured and interpreted.

2. Preparation and characterization of Au clusters

References [1–3] showed that gold and a gallium-containing $A^{III}B^{V}$ crystal in contact can react chemically upon heating to form Au clusters. Here Au clusters were prepared on the naturally oxidized (001) surface of *n*-type GaP crystals with a carrier concentration of $\sim 10^{17}\,cm^{-3}$. Before gold deposition, the *n*-GaP substrates were treated in aqueous ammonia (NH_4OH) and rinsed with deionized water. A 10 nm Au film was deposited by thermal evaporation onto the (001) surface of *n*-GaP substrates under a vacuum of 10^{-7} Torr. The resulting Au/GaP(001) structures were annealed at 400 °C for 30 min. Under these conditions, the wedge-shaped clusters consist of a mixture of gold and the intermetallic compound Au_2Ga [2,3]; they are referred to below as „Au clusters". Samples containing Au clusters were characterized using a JSM7001F scanning electron microscope (SEM; JEOL, Japan) and an Integra atomic force microscope (AFM). The characterization results are shown in Figure 1.

Figure 1, *a* shows an SEM image of the Au/GaP(001) surface after annealing. Bright, nearly rectangular regions aligned along the [110] direction of the GaP crystal are visible. They correspond to the bases of Au clusters on the GaP(001) surface, with characteristic widths of $a \cong 25-40$ nm and lengths of $2b \cong 80-110$ nm. Removing the gold by treatment in an aqueous solution of $K_4(Fe(CN)_6-CS(NH_2)$ leaves grooves elongated along [110], as seen in the AFM image of the GaP(001) surface in Figure 1, *b*. The sample characterization (Figure 1, *a, b*) and

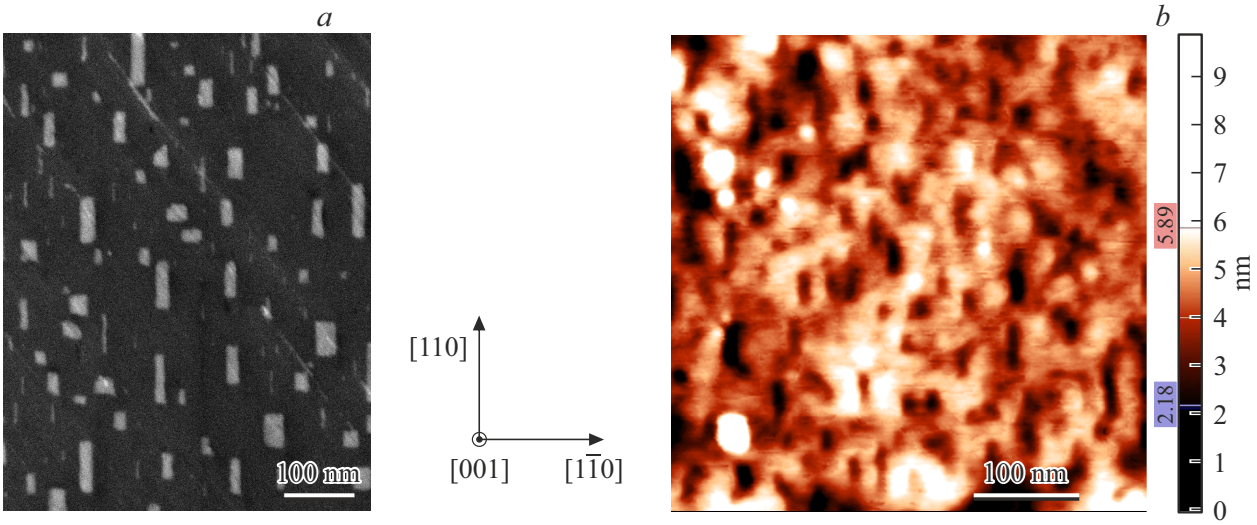


Figure 1. *a* — SEM image of the (001) GaP crystal surface after annealing a 10 nm Au overlayer in vacuum at 400 °C for 30 min. *b* — AFM image of the same sample surface after chemical removal of gold.

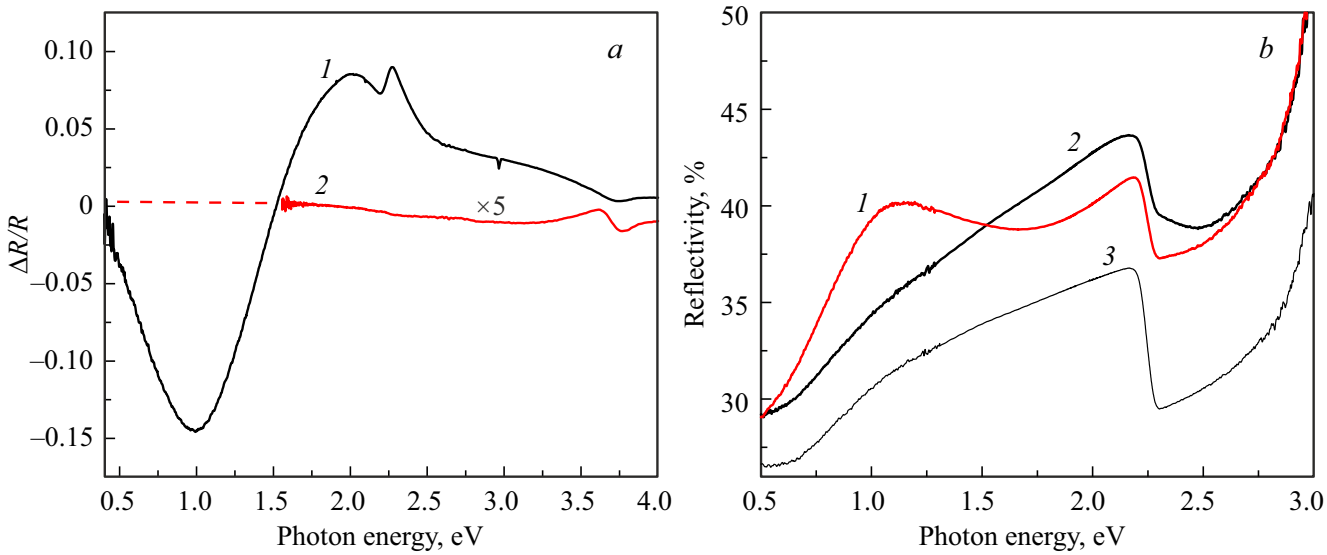


Figure 2. *a* — measured light reflectance anisotropy spectra $\Delta R/R$ of the (001) surface of an *n*-GaP crystal with Au clusters (*1*) and of *n*-GaP(001) without clusters (*2*) (multiplied by 5). *b* — normal-incidence reflectance of the *n*-GaP surface for light polarized along $\alpha = y \parallel [110]$ (*1*) and $\alpha = x[1\bar{1}0]$ (*2*) with Au clusters, and $R^{(0)}$ (*3*) without clusters.

the results of Refs. [2,3] indicate that heating Au/GaP(001) produces wedge-shaped Au nanoclusters with their tips pointing into the GaP crystal. As in Au/GaAs(001) [2], the wedge-shaped Au clusters in GaP are aligned along [110].

3. Spectroscopy of anisotropic plasmons

We assume that Au nanoclusters in Au/GaP(001) structures support anisotropic plasmons. To detect them rapidly and reliably, we use polarized-light reflectance anisotropy spectroscopy [1,2]. At normal incidence, this method measures the anisotropy signal

$$\frac{\Delta R}{R} = 2\,\frac{R_x - R_y}{R_x + R_y} \qquad (1)$$

as a function of ω. Here R_α is the reflectance for light linearly polarized along the crystallographic axis α in the GaP(001) surface plane (hereafter $x \parallel [1\bar{1}0]$ and $y \parallel [110]$, as in Figure 1). An experimentally detected anisotropy signal $\Delta R/R \neq 0$ in (1) implies $R_x \neq R_y$; this anisotropy is subsequently studied in detail by measuring reflectance for light polarized along x and y. For Au/*n*-GaP(001) structures with Au nanoclusters, the measured optical spectra of

reflectance anisotropy $\Delta R/R$ and polarized reflectance R_α are shown in Figure 2, *a, b*, respectively.

The geometry and spectra of Au clusters on a semiconductor surface are closely related to the semiconductor band structure. According to Ref. [5], GaP is transparent to photons with energies $\hbar\omega$ below the indirect interband transition threshold of 2.24 eV. It absorbs weakly up to the direct transition edge at 2.76 eV and strongly above it. The normal-incidence reflectance spectrum $R^{(0)}$ measured for the *n*-GaP crystal is shown by curve *3* in Figure 2, *b*.

Figure 2, *a* shows that anisotropy spectrum *1*, with $\max|\Delta R/R| \approx 0.15$, from the Au/GaP(001) structure differs fundamentally from spectrum *2*, with $\max|\Delta R/R| \approx 2\cdot 10^{-3}$, from the GaP surface without clusters. In the presence of Au clusters, spectrum *1* in Figure 2, *a* exhibits broad negative and positive extrema in $\Delta R/R$ at $\hbar\omega \approx 1$ and 2 eV, respectively, with a zero crossing near 1.5 eV. We attribute the resonant character and large magnitude of anisotropy signal *1* from Au/GaP(001) to anisotropic plasmons in the Au nanoclusters. According to (1), the negative feature in spectrum *1* in Figure 2, *a* corresponds to $R_{[110]} > R_{[1\bar{1}0]}$ and to plasmon polarization predominantly along the [110] elongation direction of the Au clusters, whereas the positive feature corresponds to plasmon polarization along the perpendicular direction $[1\bar{1}0]$. Near the indirect bulk transition edge at ~ 2.24 eV in *n*-GaP, a step-like feature due to donor electrons is also observed, beginning in the transparency region. Spectrum *1* of the Au/GaP(001) structure in Figure 2, *a* resembles the $\Delta R/R$ spectra of wedge-shaped Au nanoclusters formed in GaAs(001) [2].

This interpretation of the $\Delta R/R$ spectra of Au/GaP(001) is supported by the polarized reflectance spectra R_α in Figure 2, *b*. Indeed, the band peaking at 1 eV in reflectance spectrum *1* is associated with plasmons polarized in the Au clusters along the crystal [110] direction, whereas the band near 2 eV corresponds to plasmons polarized along $[1\bar{1}0]$.

4. Inhomogeneous broadening of plasmon spectra

For normal reflection of linearly polarized light from a semiconductor surface with identically oriented clusters, Eq. (1) contains

$$R_\alpha \equiv |r^{(0)} + \Delta r_\alpha|^2 \approx R^{(0)} + 2\,\mathrm{Re}\,(r^{(0)}\Delta r_\alpha^*),$$

$$\frac{\Delta R}{R} = 2\,\mathrm{Re}\left(\frac{\Delta r_x - \Delta r_y}{r^{(0)}}\right). \qquad (2)$$

Here $R^{(0)} = |r^{(0)}|^2$ is the reflectance of the optically isotropic crystal surface, and Δr_α represents the contributions of plasmons polarized along $\alpha = x, y$ in the surface plane. The expansions in (2) use $|\Delta r_\alpha| \ll |r^{(0)}|$, consistent with the observed spectra (Figure 2).

To explain the experimental spectral shapes, we use an effective-polarizability spheroidal model for plasmons in anisotropic Au nanoclusters [2]. In an individual cluster with a plasmon polarizability tensor $\hat{\chi} = \hat{\chi}' + i\hat{\chi}''$, a quasiuniform electric field $\mathbf{E}$ is assumed to induce a dipole moment $\mathbf{p} = \hat{\chi}\mathbf{E}$. For elongated Au cluster with number *n*, the components of the diagonal polarizability tensor $\chi_{\alpha\beta,n}(\omega) = \delta_{\alpha\beta}\chi_n^{(\alpha)}$ are defined along the principal axes $\alpha = x, y$ by [2,6]

$$\chi_n^{(\alpha)}(\omega - \omega_{\alpha,n}) = B_n^{(\alpha)} \frac{\omega_{\alpha,n}^2}{\omega_{\alpha,n}^2 - \omega^2 - i\omega\gamma_{\alpha,n}}. \qquad (3)$$

The frequency $\omega_{\alpha,n}$ and coefficient $B_n^{(\alpha)}$ for a plasmon polarized along α-axis depend on the semiaxis ratio b/a, where $a < b \ll c/\omega$, of the *n*th polarizable spheroid.

For normally incident light, the mean-field approximation for a crystal surface with clusters having the polarizability components (3) and mean surface density $1/l^2$ gives [2]

$$\Delta r_\alpha(\omega) = iA\sum_n \chi_n^{(\alpha)}(\omega - \omega_{\alpha,n})$$
$$= i8\pi\,\frac{\sqrt{\varepsilon_1}}{(\sqrt{\varepsilon_1}+\sqrt{\varepsilon_2})^2}\,\frac{k_0}{l^2}\,\mathrm{e}^{2ih\sqrt{\varepsilon_2}\omega/c}\sum_n \chi_n^{(\alpha)}(\omega - \omega_{\alpha,n}). \qquad (4)$$

The summation is over clusters numbered by *n* in the medium with permittivity ε_2 at a distance $h \ll c/\omega$ from the $\varepsilon_2/\varepsilon_1$ interface with the incident-light medium. Because the clusters are sparsely distributed over the surface (Figure 1), interactions between their dipolar plasmons are neglected. Surface image-force effects are assumed to be formally included in the plasmon frequencies $\omega_{\alpha,n}$. Substituting (3), (4) into (2) and using $r^{(0)} \approx -|r^{(0)}|$ for GaP over the frequency range considered yields

$$2\,\mathrm{Re}\left[|r^{(0)}|^{\pm 1}\Delta r_\alpha^*\right] \approx |r^{(0)}|^{\pm 1} C_\alpha \sum_n \frac{\omega\gamma_\alpha/2}{(\omega_{\alpha,n}-\omega)^2 + (\gamma_\alpha/2)^2} \qquad (5)$$

with $C_\alpha = \mathrm{Re}\,A \cdot \mathrm{Re}\,\overline{B}^{(\alpha)}$.

Variations in the shapes and sizes of Au clusters (Figure 1) produce inhomogeneous broadening of their plasmon oscillation lines for polarization α. For a macroscopically large ensemble of random clusters, summation over the plasmon frequencies $\omega_{\alpha,n}$ in (2)–(5) is effectively equivalent to averaging spectra (2), thereby accounting for inhomogeneous broadening. For a given polarization α, we replace the random plasmon frequencies $\omega_{\alpha,n}$, discrete in *n*, with a random variable ξ having a continuous probability density $g_\alpha(\xi - \overline{\omega}_\alpha)$, mean $\overline{\omega}_\alpha$, and normalization $\int g_\alpha(\xi - \overline{\omega}_\alpha)d\xi = 1$. Averaging the plasmon lines in (5) over their peak positions $\omega_{\alpha,n}$ is defined by the following relation (*N* is a normalization factor):

$$\frac{1}{N}\sum_n \frac{1}{(\omega - \omega_{\alpha,n})^2 + (\gamma_\alpha/2)^2} \equiv \int \frac{g_\alpha(\xi - \overline{\omega}_\alpha)}{(\omega - \xi)^2 + (\gamma_\alpha/2)^2}\,d\xi. \qquad (6)$$

Using the Cauchy distribution $g_\alpha(\xi - \overline{\omega}_\alpha) = (\delta_\alpha/2\pi)/[(\xi - \overline{\omega}_\alpha)^2 + \delta_\alpha^2/4]$ in (5)–(6) gives an

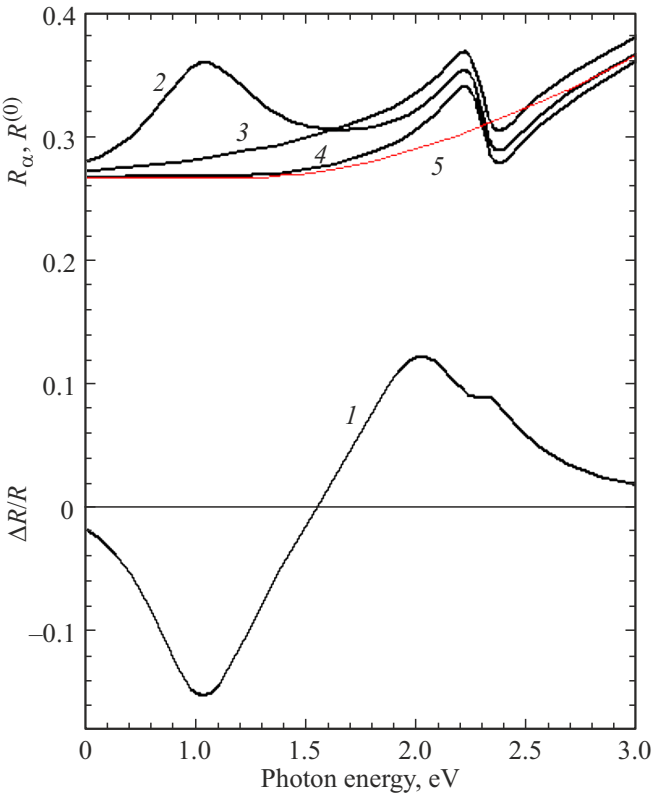


Figure 3. Inhomogeneously broadened spectra of reflectance anisotropy $\Delta R/R$ (*1*) and polarized reflectance R_y (*2*), R_x (*3*), calculated using Eqs. (7)–(9) for Au/*n*-GaP structures. Also shown are calculated normal-incidence reflectance spectra $R^{(0)}$ of *n*-GaP (*4*) and *p*-GaP (*5*) crystals without clusters. The permittivities of GaP and Au were taken from Refs. [5] and [7], respectively.

analytical estimate of the inhomogeneously broadened spectra (2):

$$\frac{\Delta R}{R}(\omega) = W_x^{(-)} L_x(\omega - \overline{\omega}_x) - W_y^{(-)} L_y(\omega - \overline{\omega}_y), \qquad (7)$$

$$R_\alpha(\omega) = R^{(0)}(\omega) + W_\alpha^{(+)} L_\alpha(\omega - \overline{\omega}_\alpha), \qquad (8)$$

$$L_\alpha(\omega - \overline{\omega}_\alpha) = \frac{\omega\Delta_\alpha/2}{(\omega - \overline{\omega}_\alpha)^2 + (\Delta_\alpha/2)^2}. \qquad (9)$$

In (7)–(8), the total widths $\Delta_\alpha = \gamma_\alpha + \delta_\alpha$ of the peaks (9) include the homogeneous γ_α and inhomogeneous δ_α contributions to plasmon line broadening. The scaling factors $W_\alpha^{(\pm)} = |r^{(0)}|^{\pm 1} C_\alpha$, with $C_\alpha \sim k_0 V/l^2$ from (5), take into account the characteristic cluster volume V and surface density $1/l^2$ in the ensemble, consistent with Figure 1.

Figure 3 shows the inhomogeneously broadened $\Delta R/R$ and R_α spectra calculated using (7)–(9) with the following fitting parameters (eV): $\hbar\overline{\omega}_y = 1$, $\hbar\overline{\omega}_x = 2$, $\hbar\gamma_y = 0.2$, $\hbar\gamma_x = 0.3$, $\hbar\delta_y = 0.4$, and $\hbar\delta_x = 0.5$. The shape of the $\Delta R/R$ spectrum, shown by curve *1* in Figure 3, agrees well with experimental spectrum *1* presented in Figure 2, *a*. The shapes of theoretical (Figure 3) reflectance spectra *2* (R_y) and 3 (R_x) also are in good agreement with the measured spectra *1* and *2* shown in Figure 2, *b*.

5. Conclusion

We have shown that annealing an Au film on the (001) surface of an *n*-GaP crystal produces wedge-shaped Au nanoclusters elongated in [110] direction. The formation of these Au clusters in Au/GaP(001) upon heating results from the chemical interaction between Au and the gallium component of the crystal, as in Au/GaAs(001). The observed polarized-light plasmon reflectance spectra of Au/GaP(001) are explained by a theory of inhomogeneous line broadening in the plasmon spectrum of an ensemble of random anisotropic Au clusters.

Conflict of interest

The authors declare that they have no conflict of interest.

References

[1] V.L. Berkovits, V.A. Kosobukin, V.P. Ulin, P.A. Alekseev, F.Yu. Soldatenkov, V.S. Levitskii. Phys. Status Solidi B, **259**, 2100394 (2022). https://doi.org/10.1002/pssb.202100394
[2] V.L. Berkovits, V.A. Kosobukin, V.P. Ulin, P.A. Alekseev, B.R. Borodin, F.Yu. Soldatenkov, A.V. Nashchekin, S.A. Khakhulin, O.S. Komkov. Surf. Sci., **742**, 122437 (2024). https://doi.org/10.1016/j.susc.2023.122437
[3] V.P. Ulin, G.V. Li, A.V. Nashchekin, V.L. Berkovits. Semicond. **59**, 381 (2025). DOI: 10.61011/SC.2025.07.62473.8680 DOI: 10.61011/FTP.2025.07.62006.8680 (In Russian).
[4] A. Ermina, N. Solodovchenko, A. Larin, V. Bolshakov, K. Prigoda, D. Markov, Y. Zharova. J. Phys. Chem. Solids, **211**, 113384 (2026). https://doi.org/10.1016/j.jpcs.2025.113384
[5] D.E. Aspnes, A.A. Studna. Phys. Rev. B, **27** (2), 985 (1983). DOI: https://doi.org/10.1103/PhysRevB.27.985
[6] V.A. Kosobukin, A.V. Korotchenkov. Phys. Sol. State **58**, 2536 (2016) DOI: 10.1134/S1063783416120131
[7] P.B. Johnson, R.W. Chrystie. Phys. Rev. B, **6** (12), 4370 (1972). DOI: https://doi.org/10.1103/PhysRevB.6.4370